Pure Appl. Geophys. 170 (2013), 1033–1046

DOI 10.1007/s00024-012-0496-2

Pure and Applied Geophysics

The 11 March 2011 Tohoku Tsunami Survey in Rikuzentakata and Comparison with Historical Events

HAIJIANG LIU,[1] TAKENORI SHIMOZONO,[2] TOMOHIRO TAKAGAWA,[3] AKIO OKAYASU,[2] HERMANN M. FRITZ,[4] SHINJI SATO,[1] and YOSHIMITSU TAJIMA[1]

Abstract—On 11 March 2011, a moment magnitude $M_w = 9.0$ earthquake occurred off the Japan Tohoku coast causing catastrophic damage and loss of human lives. In the immediate aftermath of the earthquake, we conducted the reconnaissance survey in the city of Rikuzentakata, Japan. In comparison with three previous historical tsunamis impacting the same region, the 2011 event presented the largest values with respect to the tsunami height, the inundation area and the inundation distance. A representative tsunami height of 15 m was recorded in Rikuzentakata, with increased heights of 20 m around rocky headlands. In terms of the inundation area, the 2011 Tohoku tsunami exceeded by almost 2.6 times the area flooded by the 1960 Chilean tsunami, which ranks second among the four events compared. The maximum tsunami inundation distance was 8.1 km along the Kesen River, exceeding the 1933 Showa and 1960 Chilean tsunami inundations by factors of 6.2 and 2.7, respectively. The overland tsunami inundation distance was less than 2 km. The tsunami inundation height linearly decreased along the Kesen River at a rate of approximately 1 m/km. Nevertheless, the measured inland tsunami heights exhibit significant variations on local and regional scales. A designated "tsunami control forest" planted with a cross-shore width of about 200 m along a 2 km stretch of Rikuzentakata coastline was completely overrun and failed to protect the local community during this extreme event. Similarly, many designated tsunami shelters were too low and were overwashed by tsunami waves, thereby failing to provide shelter for evacuees—a risk that had been underestimated.

Key words: Tsunami survey, historical review, inundation, run-up, Rikuzentakata, Kesen River, Tohoku tsunami, Showa tsunami, Meiji tsunami, Chilean tsunami, tsunami control forest.

1. Introduction

The 2011 Tohoku earthquake with a moment magnitude of $M_w = 9.0$ occurred at 14:46 JST (05:46 UTC) on 11 March 2011 off Japan's Miyagi Prefecture resulting from undersea thrust faulting where the Pacific plate subducts under the North American plate. It represents Japan's largest earthquake since the advent of modern instrumental recordings and ranks as the fourth largest in the world since 1900 (USGS 2011). Based on the GEONET continuous GPS network, OZAWA *et al.* (2011) reported that on land, the observed co-seismic displacements show eastward movements of up to 5.3 m and subsidence by up to 1.2 m along the coastline of the Tohoku region. Significant post-seismic deformation was also recorded. Near the hypocenter, a huge co-seismic displacement of 24 m toward ESE accompanied by 3 m uplift was measured on the seafloor (SATO *et al.* 2011). Models for this event indicated that the distribution of co-seismic fault slip exceeded 50 m in some places (SIMONS *et al.* 2011). This earthquake triggered extremely destructive tsunamis along the Japan Pacific coast, which were recognized as the predominant cause of the serious infrastructure damages and impact on coastal communities despite Japan's leading role in implementing tsunami mitigation measures. The Japan National Police Agency (JNPA 2011) estimated that 92.5 % of the overall fatalities were a result of drowning due to tsunami

[1] Department of Civil Engineering, The University of Tokyo, 7-3-1 Hongo, Bunkyo-ku, Tokyo 113-8656, Japan. E-mail: hjliu@coastal.t.u-tokyo.ac.jp; sato@coastal.t.u-tokyo.ac.jp; yoshitaji@coastal.t.u-tokyo.ac.jp

[2] Department of Ocean Sciences, Tokyo University of Marine Science and Technology, 4-5-7 Konan, Minato-ku, Tokyo 109-0075, Japan. E-mail: shimo@kaiyodai.ac.jp; okayasu@kaiyodai.ac.jp; ; ;

[3] Port and Airport Research Institute, Asia-Pacific Center for Coastal Disaster Research, 3-1-1 Nagase, Yokosuka, Kanagawa 239-0826, Japan. E-mail: takagawa-t@pari.go.jp

[4] School of Civil and Environmental Engineering, Georgia Institute of Technology, Savannah, GA 31407, USA. E-mail: fritz@gatech.edu

flooding in the Iwate, Miyagi and Fukushima Prefectures, where the bulk of the tsunami damage and death toll occurred. The measured maximum tsunami run-up height is around 40 m in Iwate Prefecture based on survey results from the Tohoku Earthquake Tsunami Joint Survey Group (Mori *et al*. 2012). Analysis of survivor videos based on LiDAR measurements allowed estimating the tsunami outflow currents of up to 11 m/s at the Kesennuma Bay narrows (Fritz *et al*. 2012). The aftermath of the 2011 Tohoku earthquake and tsunami included both humanitarian crisis and massive economic impacts.

Here, we focus on the city of Rikuzentakata in the south of Iwate Prefecture (Fig. 1). Rikuzentakata was reported to have been "wiped off the map" by the tsunami following the Tohoku earthquake (Daily Mail Reporter 2011), and was considered the most impacted city in Iwate Prefecture with 1,789 fatalities (including 234 missing presumed dead) as of 4 April 2012 (http://www.pref.iwate.jp/~bousai/). Considering the population within Rikuzentakata's flooded area of 16,640 from the statistics bureau of MIAC (http://www.stat.go.jp/info/shinsai/pdf/sinsui03.pdf), the fatality ratio to the exposed population is 10.8 %. Although the city of Rikuzentakata was completely swept away, it highlights that about 90 % of its citizens survived both the earthquake and tsunami. Rikuzentakata is located in the south of the Sanriku coast, which is a typical ria-type coast and labeled "Japan's tsunami coast". The bays of the irregular coastline tend to amplify the destructiveness of tsunami waves reaching the shores of Sanriku. Following Green's Law, many V-shaped bays along the Sanriku coast amplify the tsunami wave height during its propagation from the bay entrance to the head of the bay (Satake 2005; Shimozono *et al*. 2012).

In the last 150 years, significant tsunami disasters which impacted the Sanriku coast include: the 1896 Meiji tsunami, the 1933 Showa tsunami, the 1960 Chilean tsunami, and the 2011 Tohoku tsunami. Table 1 summarized the general information and observations at Rikuzentakata for these four events. Before the 2011 Tohoku event, the 1896 Meiji earthquake was considered the most devastating tsunami earthquake in the Sanriku region, which generated an anomalously larger tsunami than expected from its seismic waves (Kanamori 1972). Such unusual disparity between the magnitudes of an earthquake and the associated tsunami has been heavily investigated (Tanioka and Satake 1996; Hashimoto *et al*. 2009). The Meiji tsunami damage was particularly severe because the tsunami arrival coincided with a high tide level. The 1933 Showa earthquake did little damage; the associated tsunami, however, caused extensive damage and numerous casualties. The 1960 Chilean earthquake with a moment magnitude of $Mw = 9.5$ remains to date the largest earthquake instrumentally recorded. About 22 h after the earthquake, the tsunami struck Japan, which is about 17,000 km away from the Chilean epicenter, and caused unexpected damage, although the offshore tsunami wave height was low in comparison to the previous two Japanese cases (Iwate Prefecture 1969). The 2011 Tohoku earthquake tsunami, however, eclipsed all the existing tsunami records and damage extents in Rikuzentakata. The inundation area for the 2011 Tohoku tsunami is estimated to 13.45 km^2 in the city of Rikuzentakata, thereby significantly eclipsing the 1.56, 1.34 and 5.25 km^2 for the Meiji, Showa and Chilean tsunamis, respectively (Table 1). An early overview of the 2011 Tohoku tsunami damage along the Sanriku coast has been summarized by Liu *et al*. (2011).

2. *Post-Tsunami Reconnaissance*

In the immediate aftermath of the 2011 Tohoku earthquake, post-tsunami field survey teams were deployed to the city of Rikuzentakata during the two time periods of 26–29 March and 9–11 April 2011. The target area covered the region surrounding the Hirota Bay, starting from the Ozaki Cape on the Karakuwa Peninsula in the west, advancing into the bay head section of Rikuzentakata's urban area, and ending at the Hirota Cape on the Hirota Peninsula in the east (Fig. 1). Similar to previous tsunami surveys (Hokkaido Tsunami Survey Group 1993; Borrero 2005; Liu *et al*. 2005), the tsunami inundation and run-up heights were measured. The inundation height is defined as the local tsunami height above the sea level excluding astronomical tide, and the run-up height is determined at the elevation of the maximum

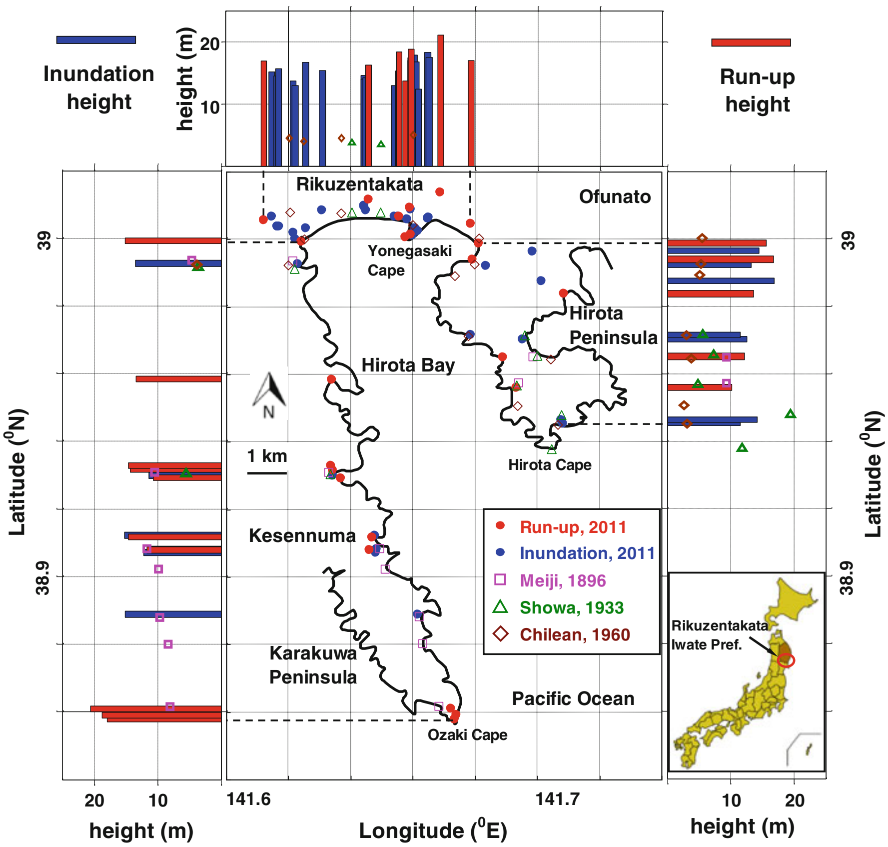

Figure 1
Tsunami survey results along the Hirota Bay. Bar graphs are for measured tsunami inundation (*blue*) and run-up (*red*) heights of the 2011 Tohoku tsunami, in which historical records of tsunami heights for the 1896 Meiji (*magenta square*), the 1933 Showa (*green triangle*) and the 1960 Chilean events (*brown diamond*) are also superimposed

Table 1

Historical earthquake and tsunami information in Rikuzentakata

Event	Date	Earthquake magnitude	Representative tsunami height (m)	Inundation area (km^2)	References
Meiji	15 June 1896	7.2	~4.6	1.56	Matsuo (1933) and MHA (1934)
Showa	3 March 1933	8.1	3.5–3.8	1.34	Matsuo (1933) and MHA (1934)
Chilean	22 May 1960	9.5	4.5–5.0	5.25[a]	Iwate Prefecture (1969)
Tohoku	11 March 2011	9.0	~15.0	13.45	JAXA (2011)

[a] Estimated from the inundation map in Iwate Prefecture (1969)

inundation (Mori *et al*. 2012). Similarly, the tsunami uprush characteristics along the rivers were also documented. In total, 86 data points were recorded and tabulated in Appendix Table 2.

The surveying equipment used in the field includes: Real-time Kinematic GPS (RTK-GPS), Trimble GPS, laser range finders and survey rods. All measured tsunami height data were converted into the T.P. (Tokyo Peil) standard. Elevation of T.P. zero corresponds to the average water level at the Tokyo Bay, which is a standard geodetic datum used in Japan. The tsunami inundation and run-up heights were detected from watermarks such as rafted debris, wracklines, mudlines on walls or windows of remaining buildings, broken branches and bark damage on trees. Certain watermarks were confirmed by interviews with eyewitnesses.

3. Result and Discussion

Apart from the offshore tsunami wave characteristics, e.g., incident wave length and period, the tsunami height distribution around a bay is also affected by various topographic factors, such as the orientation, shape, length and bathymetry of a bay. In addition, the tsunami may be resonated if the natural frequency of the bay matches the tsunami wave period, which locally amplifies the wave height and exacerbates damage (SATAKE and KANAMORI 1991; MUNGER and CHEUNG 2008). A general discussion on propagation and inundation characteristics of the 2011 Tohoku tsunami on the central Sanriku Coast is presented by SHIMOZONO *et al*. (2012), who focused on the influence of the orientation and the bathymetric slope of a bay.

The measured tsunami inundation and run-up heights along the shoreline of the Hirota Bay show a representative tsunami height of about 15 m (Fig. 1). Given the U-shape of Hirota Bay, the funneling effect (tsunami amplification in a V-shaped bay due to energy concentration) from the entrance to the head of the bay was widely absent. Relatively large run-up heights around rocky cape tips were detected, e.g., about 20 m at the Ozaki Cape and the Yonegasaki Cape. This is ascribed to the steep rocky coastlines and refraction effects of tsunami waves. The wave energy converged on the protruding capes, resulting in the locally high tsunami run-up.

Taking into account historical recordings of the tsunami heights for the 1896 Meiji tsunami (MATSUO 1933), the 1933 Showa tsunami (MATSUO 1933) and the 1960 Chilean tsunami (CFICT 1961; IWATE PREFECTURE 1969), tsunami heights in Rikuzentakata are absolutely the highest for the 2011 Tohoku event followed by the 1896 Meiji event (Fig. 1). As for the three earlier tsunamis, it remains unclear whether the documented tsunami heights represent inundation or run-up heights. Presumably those tsunami heights may be inundation heights considering the limitations in measuring instruments at the time. In terms of the 1933 Showa event, the tsunami wave period is relatively short, around 10 min (MATSUO 1933). The 1933 tsunami showed a bore-like waveform, penetrated with highly turbulent motion and caused severe damage to coastal infrastructures (CFICT 1961). The 1933 tsunami wave height was relatively large at the bay entrance, e.g., 11.8 m at the Hirota Cape, and decreased to 3.5 m at the head of the bay. In contrast, the 1960 Chilean tsunami presented an inverse scenario with 2–3 m tsunami heights at the bay entrance increasing towards the head of the bay to about 4–5 m, which led to a wider and deeper inundation area than the area flooded by the Meiji or Showa tsunamis (Fig. 2). The 1960 Chilean event was characterized by an extremely large source area resulting in extraordinarily long tsunami wave periods (PLAFKER and SAVAGE 1970; KANAMORI 1977). Further considering the transoceanic nature of the Chilean tsunami with a propagation around 40 % of the Earth's circumference from the epicenter to the Japan Coast, the short wave components were gradually dissipated with only long wave components remaining. Consequently, the tsunami wave lengths recorded along the Japan Coast were fairly long with predominant tsunami wave periods of 60–80 min (CFICT 1961). The rise and fall in water level due to the 1960 tsunami occurred very gradually and quietly. The rupture of the 2011 Tohoku-Oki megathrust earthquake consisted of a small initial phase deep rupture, extensive shallow rupture (dynamic overshoot), and continuing deep rupture (IDE *et al*. 2011). Two-step tsunami waveforms were recorded by ocean-bottom pressure sensors and GPS wave gauges: a gradual increase of sea level due to the slip on the plate interface, followed by an impulsive tsunami wave triggered by the large slip along the trench axis (FUJII *et al*. 2011). As a result, the tsunami waveforms recorded at the offshore of the Sanriku region contained an extreme peak with a short wave period of about 8 min superposed on an elevated water level with a longer 30 min wave period. These tsunami-generation mechanisms and the relevant offshore tsunami waveforms, together with the local topographic and bathymetric features of the Hirota Bay, lead to the uniform spatial distribution of the 2011 Tohoku tsunami heights around Hirota Bay.

An inundation comparison in Rikuzentakata demonstrates that the inundation area of the 2011 Tohoku tsunami is by far the largest and exceeds by a factor of almost 2.6 the area inundated by the 1960 Chilean tsunami (Fig. 2; Table 1). Several unique observations were made after the 2011 Tohoku tsunami attack. The 2011 event represents the first time a tsunami wave passed through the narrow throat cross-section A–A channeling the Kesen River route between mountain slopes (Fig. 2). Lee-side residents cannot view the sea directly, and generally consider themselves mountain people despite residing in a location with a fairly low elevation. Unfortunately, this time the powerful tsunami thrust through the narrow section A–A located 2.6 km upriver, caused devastating destruction and casualties with tsunami waves fanning inland across the low-lying ground up to 8.1 km upriver. In addition, for the first time, the entire area at the base of the Hirota Peninsula was within the tsunami inundation zone, converting the southern region of the Hirota Peninsula into a temporally isolated island during the tsunami flooding. Along the Yahagi River, the inundation area was larger on the north side as the northward propagating tsunami wave changed its direction to WSW after the confluence of the Kesen and Yahagi Rivers. The inundation area extended far inland along the river routes for all four events, e.g., the Kesen River and the Osabe River in Fig. 2. This is attributed to the upriver tsunami propagation and lateral overflowing of relatively low riverbanks. Therefore, countermeasures against upriver tsunami flooding are particularly important for the protection of local communities.

A spatially dense survey of tsunami heights through the urban area of Rikuzentakata resolved the detailed overland tsunami characteristics (Fig. 3). Comparison between the background satellite images of Fig. 2 (pre-tsunami) and Fig. 3 (post-tsunami) shows a massive landward retreat of the shoreline after the tsunami attack. The land loss is attributed to

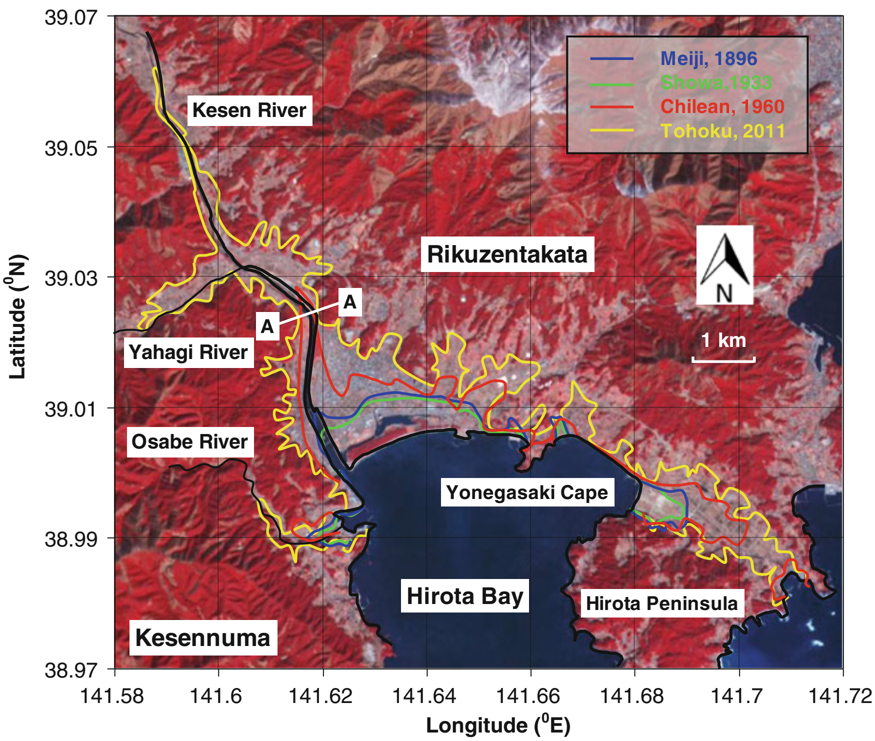

Figure 2

Comparison of inundation areas for the four historical tsunamis in Rikuzentakata. *Black lines* indicate the shoreline and river route before the tsunami. Inundation areas for the 1896 Meiji tsunami (*blue*), the 1933 Showa tsunami (*green*), the 1960 Chilean tsunami (*red*) and the 2011 Tohoku tsunami (*yellow*) are presented with colored lines identifying the extent of inundation. Background is the ASTER satellite image recorded on 1 March 2007 co-seismic subsidence as well as tsunami uprush and drawdown erosion. A co-seismic subsidence of approximately 0.65 m was measured at Rikuzentakata by the Geospatial Information Authority of Japan. In the aftermath of the tsunami, a large collection of debris was floating on the east side of the Hirota Bay head (Fig. 3). The maximum tsunami inundation distance of 8.1 km upriver from the river mouth along the Kesen River, significantly exceeds the previous events, e.g., 1.3 km for the 1933 Showa tsunami and 3.0 km for the 1960 Chilean tsunami (CFICT 1961). Similarly, the maximum tsunami uprush along the Yahagi River measured 6.7 km. Tsunami inundation distances along the river route are much larger than the maximum overland inundation distances, e.g., 1.9 km along the survey line L2 in Fig. 3. Similar 15 km upriver inundation along the Maule River was also reported during the 2010 Chile tsunami (FRITZ *et al*. 2011). This is ascribed to the relatively low elevation along the river route, as well as the large overland bottom friction induced by remnant houses and buildings which act as wave energy dissipaters along the tsunami inland propagation.

Figure 4a shows that the tsunami height is slightly larger on the east side of the Kesen River. The inundation height at the Yahagi River is almost the same as along the main river route in terms of the corresponding distance from the Kesen River mouth. With increasing tsunami upriver propagation, the tsunami height gradually decreases towards the river's upper reaches. The decay is almost linearly proportional to the travelling distance along the river route at a rate of 1 m/km. On the contrary, the tsunami heights gradually increase in the urban area along the survey line L1 as shown in Fig. 4b. This increase of tsunami heights from 14.5 m near the shoreline to 18.5 m at the run-up location is accompanied by an abrupt change in the topographic ground elevation. Along the survey line L2, the tsunami height remains relatively uniform at 15.5 m, while the topographic ground elevation gradually increases by 13.5 m along the survey transect. A decreasing trend is found along the survey line L3, which is adjacent to the Kesen River and follows the same trend as the tsunami height distribution along the river route (Fig. 4a). As for these three transects, the overland flow depth presented maximum values of approximately 15 m near the shoreline, followed by landward decays. Considering the longshore variation in the inland area (more than 1,000 m away from the shoreline in Fig. 4b), the topographic ground elevations increase eastwardly from line L3 to line L1. The recorded tsunami heights also increased eastwards in accordance with the underlying topographic features along the WE direction.

Figure 5 shows the pre- and post-tsunami situations in Rikuzentakata. Comparing with the satellite image recorded before the tsunami (Fig. 5a), an aerial post-tsunami photograph shown in Fig. 5b dramatically reveals the devastating tsunami destruction in Rikuzentakata. Most of the sand spit originally located at the east side of the Kesen River mouth was eroded after the tsunami attack. These sands were transported by the tsunami and may be deposited in the inland flood zone or washed into the bay by the subsequent tsunami outflow. For tsunami mitigation purposes, a coastal forest was planted and maintained over the past 300 years on the sand spit with more than 70,000 mature pine trees before tsunami onslaught as shown in Fig. 5a. This 2 km longshore tsunami control forest with a width of about 200 m was supposed to act similar to an artificial breakwater protecting the inland communities from storm waves and tsunami surges. Earlier studies pointed out the effectiveness of coastal forests at reducing coastal flooding due to the tsunami events and cyclone storm waves (SHUTO 1987; DANIELSEN *et al*. 2005; TANAKA *et al*. 2007; FRITZ *et al*. 2009). Unfortunately, the coastal forest in Rikuzentakata failed to protect the local residents this time. Almost all pine trees were washed away by the 15 m high tsunami wave and became floating debris impacting buildings as battering rams (Fig. 6d). The sole surviving pine tree highlighted in Figs. 5b and 6e, named "the tree of hope", was regarded as a symbol of reconstruction by local residents. Accordingly, the conventional understanding of the tsunami mitigation provided by coastal forests should be re-evaluated, especially for such extreme tsunami events.

The 15 m high tsunami tore down all structures in Rikuzentakata except for several reinforced concrete buildings (Fig. 5), e.g., the seven-floor Capital Hotel, a building of the roadside station along the national road No. 45, the city's indoor sports arena and the

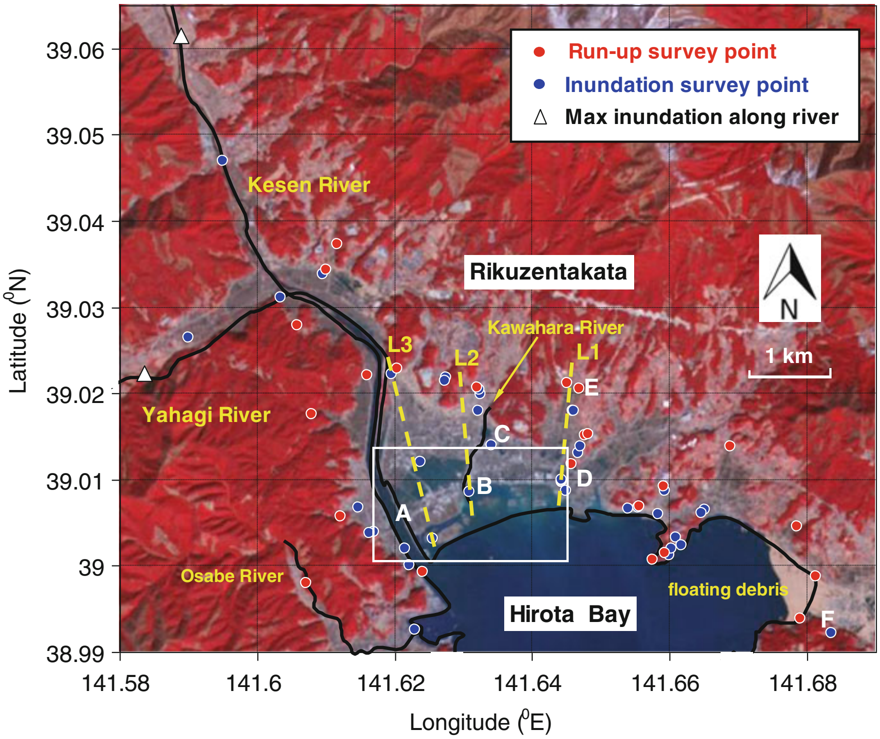

Figure 3
Field survey in the Rikuzentakata urban area and along the Kesen River. *Dots* show the locations where tsunami heights are measured. *Triangles* mark the inundation limits along the Kesen and the Yahagi Rivers. *Black lines* indicate the shoreline and river route before the tsunami. Background is the ASTER satellite image recorded on 14 March 2011. The *rectangle* indicates the region shown in Fig. 5b

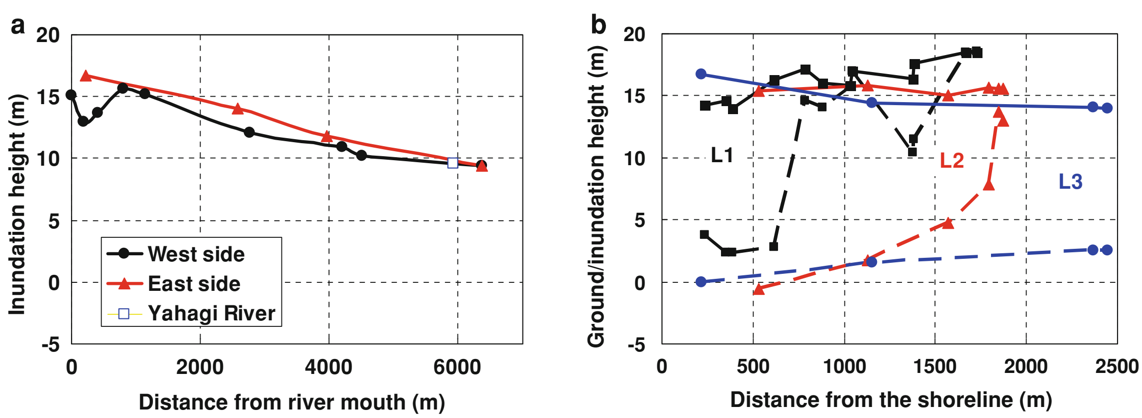

Figure 4
Overland tsunami height spatial distribution. **a** Tsunami inundation heights along both sides of the Kesen River, as well as the Yahagi River. **b** Measured tsunami height distribution (*solid lines*) and the corresponding ground elevation (*dashed lines*) along three cross-shore directional survey lines, *L1*, *L2* and *L3* indicated in Fig. 3

city hospital. A close-up view of tsunami impact on these structures is presented in Fig. 6a–d. Tsunami inundation heights were documented on these buildings. The railway of the Ofunato Line, including the Rikuzentakata Station, was completely destroyed and most broken railroad tracks could not even be located during our field survey. The triangle-shaped building of the roadside station was designated as a tsunami

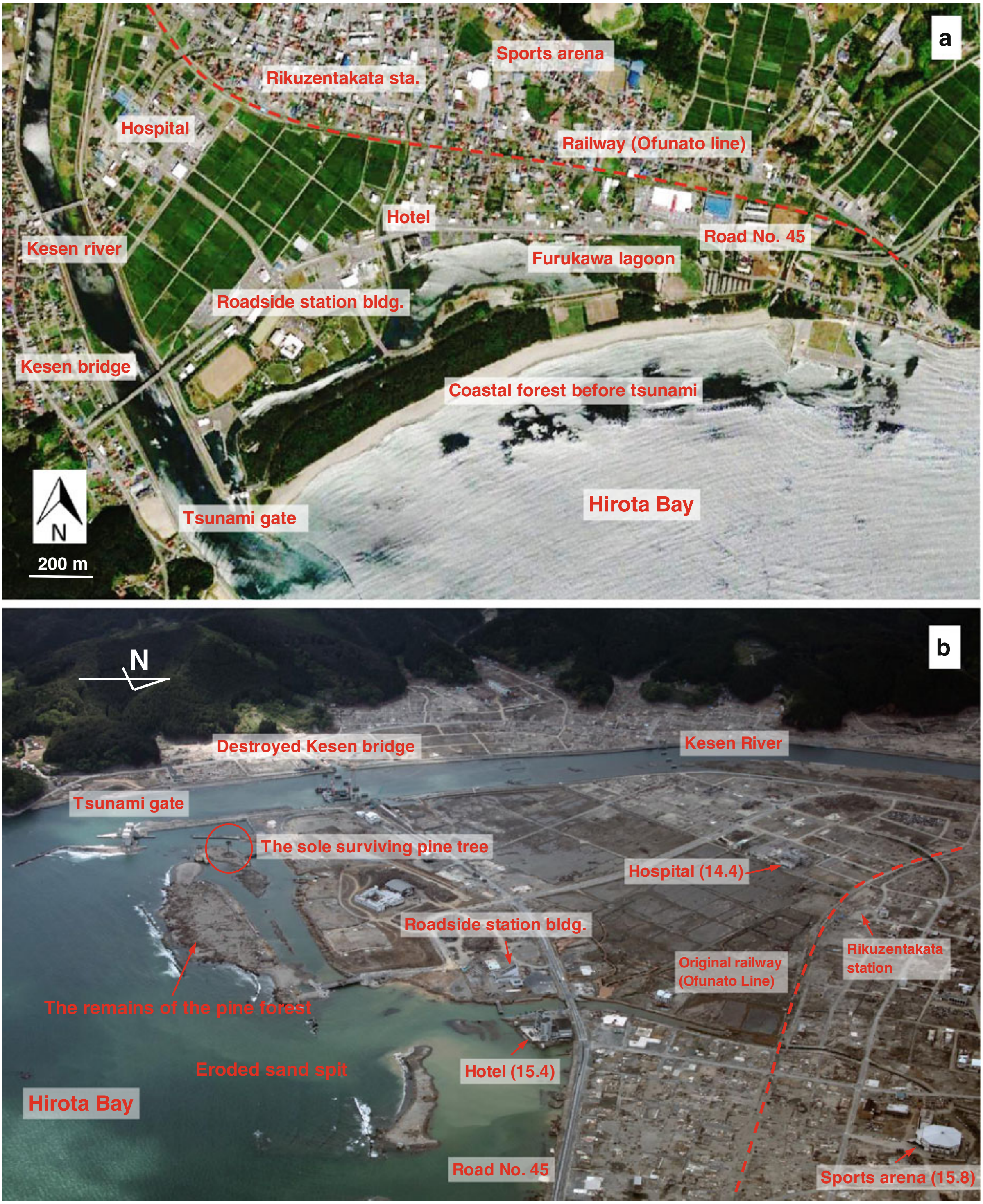

Figure 5

Comparison of the pre- and post-tsunami situations in Rikuzentakata. **a** Pre-tsunami satellite image of the city of Rikuzentakata. Image was recorded on 23 July 2010 (Photo credit: GeoEye). **b** Aerial photograph of the city of Rikuzentakata after the tsunami attack. Image was recorded on 25 May 2011 (Photo credit: Geospatial Information Authority of Japan). *Numbers* in brackets indicate the measured tsunami inundation height at these locations. The *dashed line* represents the railway route of the Ofunato Line evacuation building featuring a unique design, with exterior stairs and a series of platforms on the seaward slope (Fig. 6b). Although the building structurally survived the tsunami, only the two or three uppermost stairs were above the highest tsunami water level and provided shelter. All evacuees staying inside the building, possibly avoiding the winter weather outside, lost their lives. Only a few evacuees managed to climb to the top of the building and survived the tsunami. Prior to this tsunami event, the city's indoor sports arena was also designated as a tsunami shelter. Unfortunately, only three out of about 100 evacuees were able to survive the tsunami here since the violent tsunami almost reached the roof of the arena. The significant tsunami impact force toppled the massive backside wall of the sports arena as a complete unit, without crumbling into pieces (Fig. 6c). Floating pine tree trunks impacted the front of the city hospital, which is located 1 km inland from the coastal forest (Fig. 6d). The Furukawa lagoon adjacent to the east of the Kesen River mouth was armed with a tsunami gate, which was closed after the earthquake but designed for events an order of magnitude smaller and was massively overwashed

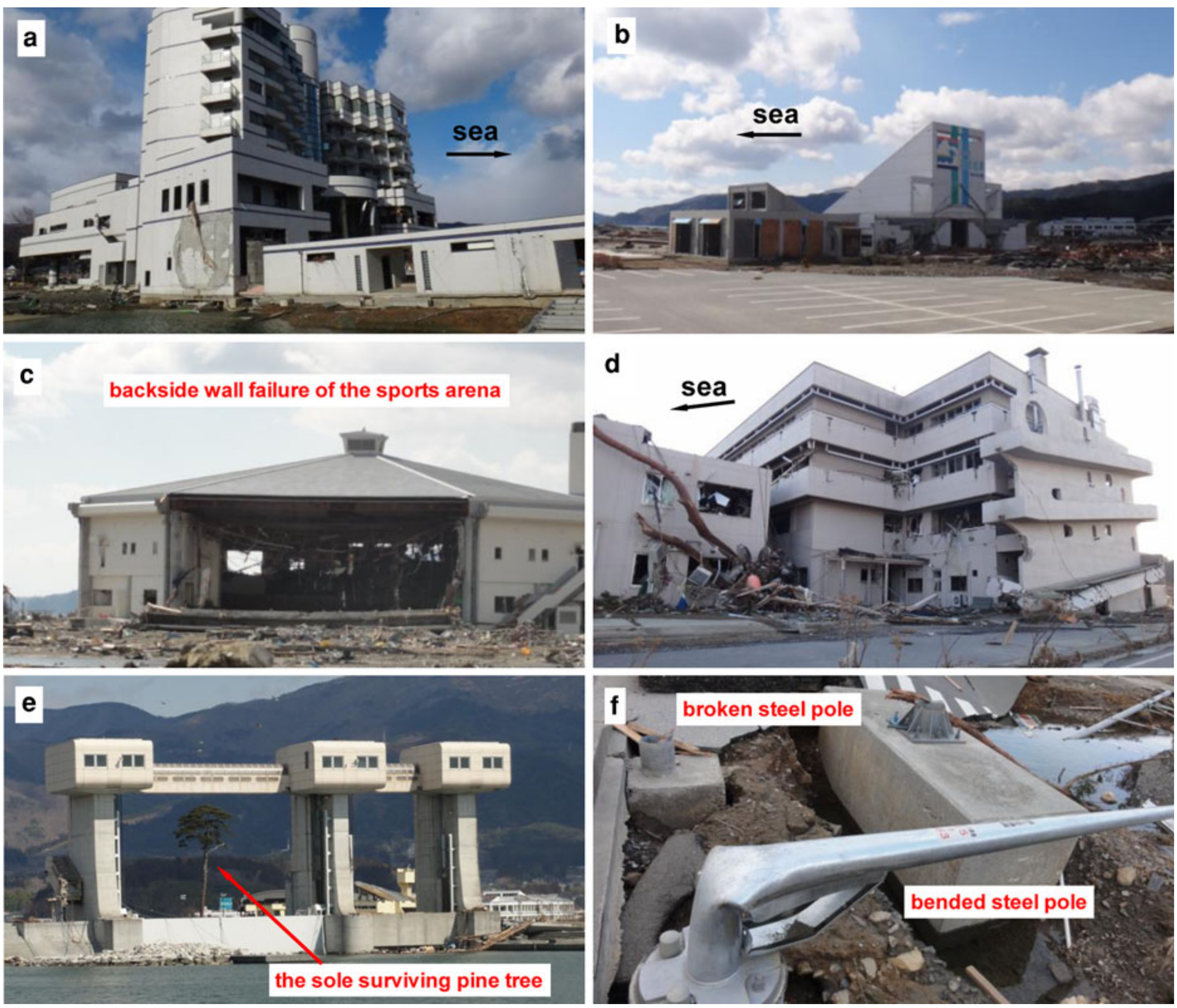

Figure 6
A close-up view of the tsunami impact on various structures in Rikuzentakata. **a** The seven-floor Capital Hotel. **b** The tsunami evacuation building of the roadside station. **c** Backside wall failure of the city's indoor sports arena. **d** The city hospital. **e** The tsunami gate at the entrance to Furukawa lagoon with the sole surviving pine tree behind. **f** Bended and broken steel poles

with only the reinforced concrete frame remaining after the event (Fig. 6e). The sole surviving pine tree stands behind this tsunami gate. Figure 6f shows several bended or broken steel poles beside the national road No. 45. These hollow steel poles with a bottom diameter around 20 cm fell down landwards. Investigation on poles or steel bars falling direction indicated that most of them failed during the tsunami uprush phase.

Here, we further select several representative locations to discuss post-tsunami observation scenarios in Rikuzentakata (Fig. 7). The Kesen Bridge, 0.66 km upstream from the river mouth, was completely submerged by the tsunami and destroyed with only bridge piers remaining after the event (Fig. 7a, also Fig. 5b). Overflow of the collapsed riverbanks was also confirmed. In Fig. 7b, significantly oblique subsidence of a two-story building occurred due to the tsunami outflow scouring as the water funneled to the low-elevation channels, such as the Kawahara River which has no high riverbank. Severe damage caused by the tsunami outflow was demonstrated here although earlier studies assumed small outflow velocities (Imamura *et al*. 2008; Furumura *et al*.

Figure 7

Post-tsunami field observation scenarios in Rikuzentakata. **a** Remaining piers of the Kesen Bridge and the broken riverbanks at location A. **b** A sunk building after tsunami outflow scouring next to the Kawahara River at location B. **c** A relocated and overturned boulder in front of the city's indoor sports arena at location C. **d** Tsunami inundation height and damages for two five-story buildings at location D. **e** A maximum tsunami run-up height at location E. **f** A damaged temple at location F (all locations are indicated in Fig. 3)

2011). In our field survey, a relocated and overturned boulder was found deposited in front of the city's indoor sports arena (Fig. 7c). This giant granite boulder has a dimension of 3.6 m (length) × 2.0 m (height) × 2.1 m (width), and was transported 35 m inland from its original location. Further landward boulder movement could be expected without impediment from the sports arena. Such boulder transport by tsunami waves has been widely reported (Kato and Kimura 1983; Nott 2003; Frohlich *et al.* 2009). Figure 7d shows the post-tsunami situation of two five-story buildings located 360 m inland from the shoreline. All the balcony fences below the fifth floor of the seaside front building were broken and the measured local inundation height is 14.6 m. In contrast, damage on the landward second building was minor with even most balcony fences remaining intact. These striking differences in post-tsunami damage levels are attributed to the protective role provided by the front building. Figure 7e illustrates a detected tsunami run-up point, marked by a roadside wrackline, located 1.7 km inland from the shoreline with a local ground elevation of 18.5 m corresponding to a run-up height. Figure 7f shows that an ancient temple which safely survived aforementioned three historical tsunami disasters according to local residents, was destroyed by the 2011 event. Eyewitness interviews revealed that a number of residents attempted to evacuate to such ancient temples and shrines to seek shelter from the tsunami based on their ancestral experience, which proved to be life saving in the 2007 Solomon Islands tsunami (Fritz and Kalligeris 2008). Unfortunately, the extreme tsunami caused unexpected fatalities at such tsunami shelters this time.

4. Conclusion

Two weeks after the 11 March 2011 Tohoku earthquake tsunami, we conducted field surveys in the city of Rikuzentakata in Japan's Iwate Prefecture. Comparing with the 1896 Meiji, the 1933 Showa and the 1960 Chilean tsunamis, the 2011 Tohoku tsunami presents the largest values with respect to the tsunami height, the inundation area and the inundation distance. Relatively uniform tsunami heights were recorded along the Hirota Bay with a representative tsunami height of 15 m and an increased height of 20 m at rocky cape tips. In terms of the inundation area, the 2011 Tohoku tsunami exceeded by almost 2.6 times the area flooded by the 1960 Chilean tsunami, which locally ranks second in this regard. The maximum tsunami inundation distance along the Kesen River of 8.1 km from the river mouth, exceeded by factors of 6.2 and 2.7 records of the 1933 Showa and the 1960 Chilean tsunami events. The tsunami overland inundation distance was less than 2 km. Tsunami inundation height linearly decreased along the Kesen River at a rate of 1 m/km. Following the complex regional topography, the spatial variation of tsunami overland inundation heights exhibits local characteristics. In general, the inland tsunami height gradually increased eastwards.

Several tsunami characteristics in Rikuzentakata were identified during the 2011 Tohoku tsunami event, e.g., the significant tsunami inundation even in the riverine plains behind mountains and the temporary island forming connection between the tsunami inundation pincers at the base of the Hirota Peninsula. Unfortunately, a 2 km longshore coastal pine forest with a width of 200 m was completely washed away and failed to protect the local community during this event. Similarly, many designated tsunami shelters, e.g., the tsunami evacuation buildings, the city's indoor sports arena and the ancient temples, were within the massive tsunami flood zone. Many evacuation buildings were designated based on smaller tsunami scenarios resulting in flooding of upper floors thereby failing to save the lives of many evacuees. Such information is extremely important for the forthcoming reconstruction works, as well as the planning of future tsunami disaster prevention and mitigation.

Acknowledgments

The post-tsunami survey was financially supported by the JST J-RAPID project through the Program of "Study on the 2011 Tohoku Tsunami propagation, tsunami nearshore behavior, and tsunami mitigation from coastal structures". The University of Tokyo survey team (H.L., S.S. and Y.T.) was also supported by the Nippon Foundation through the program for the Basis of Marine Affairs. H.M.F. was supported by NSF RAPID award CMMI-1135768.

Appendix

See Table 2

Table 2

Post-tsunami field survey dataset in Rikuzentakata

No.	Latitude (°N)	Longitude (°E)	Inundation (I)/ run-up (R)	Height (m)	Date	Group[a]
1	39.009694	141.644278	I	14.6	Mar 27/28	TUMST/UT
2	39.009833	141.644250	I	14.6	Mar 27/28	TUMST/UT
3	39.010028	141.644306	I	14.0	Mar 27/28	TUMST/UT
4	39.008639	141.644889	I	14.2	Mar 27/28	TUMST/UT
5	39.013056	141.646778	I	17.2	Mar 27/28	TUMST/UT
6	39.013889	141.647028	I	16.0	Mar 27/28	TUMST/UT
7	39.017972	141.645861	I	16.4	Mar 27/28	TUMST/UT
8	39.018028	141.646056	I	17.6	Mar 27/28	TUMST/UT
9	39.008500	141.630944	I	15.4	Mar 27/28	TUMST/UT
10	39.014000	141.634069	I	15.8	Mar 27/28	TUMST/UT
11	39.012000	141.623694	I	14.4	Mar 27/28	TUMST/UT
12	39.022250	141.619556	I	14.1	Mar 27/28	TUMST/UT
13	38.992528	141.622944	I	13.5	Mar 27/28	TUMST/UT
14	39.033833	141.609583	I	11.3	Mar 27/28	TUMST/UT
15	39.026528	141.590056	I	9.6	Mar 27/28	TUMST/UT
16	39.031167	141.603389	I	10.2	Mar 27/28	TUMST/UT
17	39.046972	141.595083	I	9.4	Mar 27/28	TUMST/UT
18	39.021806	141.627500	I	15.5	Mar 27/28	TUMST/UT
19	39.021472	141.627278	I	15.4	Mar 27/28	TUMST/UT
20	39.017972	141.632222	I	15.0	Mar 27/28	TUMST/UT
21	39.019917	141.632472	I	15.7	Mar 27/28	TUMST/UT
22	39.020389	141.632306	I	15.6	Mar 27/28	TUMST/UT
23	38.996486	141.698472	I	14.5	Mar 27/28	TUMST/UT
24	38.987611	141.701361	I	16.8	Mar 27/28	TUMST/UT
25	38.992222	141.683611	I	13.2	Mar 27/28	TUMST/UT
26	39.011778	141.645667	R	16.3	Mar 27/28	TUMST/UT
27	39.015139	141.647750	R	15.8	Mar 27/28	TUMST/UT
28	39.015250	141.648111	R	17.0	Mar 27/28	TUMST/UT
29	39.020528	141.646917	R	18.5	Mar 27/28	TUMST/UT
30	39.021139	141.645056	R	18.5	Mar 27/28	TUMST/UT
31	39.022906	141.620306	R	14.0	Mar 27/28	TUMST/UT
32	38.999278	141.624056	R	15.1	Mar 27/28	TUMST/UT
33	38.958361	141.633889	R	13.4	Mar 27/28	TUMST/UT
34	39.034361	141.610111	R	12.4	Mar 27/28	TUMST/UT
35	39.037333	141.611694	R	12.4	Mar 27/28	TUMST/UT
36	39.020611	141.631972	R	15.6	Mar 27/28	TUMST/UT
37	38.983789	141.708689	R	13.6	Mar 27/28	TUMST/UT
38	38.993889	141.679083	R	16.7	Mar 27/28	TUMST/UT
39	38.888873	141.661781	I	15.1	Apr 10/11	TUMST/GIT
40	38.912285	141.647776	I	15.2	Apr 10/11	TUMST/GIT
41	38.907112	141.648209	I	12.2	Apr 10/11	TUMST/GIT
42	38.908108	141.648524	I	11.6	Apr 10/11	TUMST/GIT
43	38.929872	141.634317	I	11.4	Apr 10/11	TUMST/GIT
44	39.006644	141.654055	I	13.0	Apr 10/11	TUMST/GIT
45	39.006725	141.655355	I	15.3	Apr 10/11	TUMST/GIT
46	39.005945	141.658308	I	13.6	Apr 10/11	TUMST/GIT
47	39.008745	141.659305	I	17.0	Apr 10/11	TUMST/GIT
48	39.003267	141.660893	I	16.8	Apr 10/11	TUMST/GIT

Table 2 *continued*

No.	Latitude (°N)	Longitude (°E)	Inundation (I)/ run-up (R)	Height (m)	Date	Group[a]
49	39.001232	141.660012	I	14.2	Apr 10/11	TUMST/GIT
50	39.001997	141.660354	I	17.9	Apr 10/11	TUMST/GIT
51	39.002347	141.661694	I	12.4	Apr 10/11	TUMST/GIT
52	39.003171	141.625559	I	16.7	Apr 10/11	TUMST/GIT
53	39.000034	141.622182	I	13.0	Apr 10/11	TUMST/GIT
54	39.002010	141.621526	I	13.7	Apr 10/11	TUMST/GIT
55	39.003855	141.616912	I	15.7	Apr 10/11	TUMST/GIT
56	39.003772	141.616323	I	14.5	Apr 10/11	TUMST/GIT
57	39.006795	141.614677	I	15.2	Apr 10/11	TUMST/GIT
58	39.006509	141.665133	I	17.5	Apr 10/11	TUMST/GIT
59	39.006113	141.664709	I	18.3	Apr 10/11	TUMST/GIT
60	38.860889	141.672442	R	20.6	Apr.10/11	TUMST/GIT
61	38.859058	141.674149	R	18.8	Apr 10/11	TUMST/GIT
62	38.857911	141.673537	R	18.0	Apr 10/11	TUMST/GIT
63	38.911676	141.646952	R	14.6	Apr.10/11	TUMST/GIT
64	38.907889	141.646067	R	11.7	Apr 10/11	TUMST/GIT
65	38.929181	141.636838	R	10.7	Apr 10/11	TUMST/GIT
66	38.932900	141.633647	R	14.6	Apr 10/11	TUMST/GIT
67	38.931620	141.634272	R	14.3	Apr 10/11	TUMST/GIT
68	38.929604	141.627485	R	16.5	Apr 10/11	TUMST/GIT
69	38.997968	141.607148	R	14.7	Apr 10/11	TUMST/GIT
70	38.998756	141.681246	R	15.6	Apr 10/11	TUMST/GIT
71	39.006840	141.655547	R	18.4	Apr 10/11	TUMST/GIT
72	39.009250	141.659131	R	17.4	Apr 10/11	TUMST/GIT
73	39.000716	141.657546	R	13.7	Apr 10/11	TUMST/GIT
74	39.001515	141.659359	R	18.8	Apr 10/11	TUMST/GIT
75	39.005688	141.612162	R	16.9	Apr 10/11	TUMST/GIT
76	39.017541	141.607954	R	18.4	Apr 10/11	TUMST/GIT
77	39.022058	141.615982	R	12.1	Apr 10/11	TUMST/GIT
78	39.027949	141.605854	R	10.9	Apr 10/11	TUMST/GIT
79	39.013890	141.668804	R	21.1	Apr 10/11	TUMST/GIT
80	39.004516	141.678590	R	17.0	Apr 10/11	TUMST/GIT
81	38.945472	141.708250	I	11.5	Apr 10	UT
82	38.946444	141.707778	I	14.2	Apr 10	UT
83	38.970278	141.695444	I	12.5	Apr 10	UT
84	38.971583	141.678722	I	11.5	Apr 10	UT
85	38.955944	141.693417	R	10.2	Apr 10	UT
86	38.965167	141.689000	R	12.2	Apr 10	UT

TUMST Tokyo University of Marine Science and Technology, *GIT* Georgia Institute of Technology, *UT* The University of Tokyo

References

BORRERO, J.C. (2005). *Field data and satellite imagery of tsunami effects in Banda Aceh*. Science, *308*, 1596.

CFICT, The Committee for Field Investigation of the Chilean tsunami of 1960 (1961). *Report on the Chilean Tsunami of May 24, 1960, as observed along the coast of Japan*. p. 397.

Daily Mail Reporter (2011). http://www.dailymail.co.uk/news/article-1365397/Japan-earthquake-tsunami-The-moment-apocalyptic-waves-drown-Rikuzentakata.html.

DANIELSEN, F., SØRENSEN, M.K., OLWIG, M.F., SELVAM, V., PARISH, F., BURGESS, N.D., HIRAISHI, T., KARUNAGARAN, V.M., RASMUSSEN, M.S., HANSEN, L.B., QUARTO, A. and SURYADIPUTRA, N. (2005). *The Asian tsunami: A protective role for coastal vegetation*. Science, *310*, 643.

FRITZ, H.M. and KALLIGERIS, N. (2008). *Ancestral heritage saves tribes during 1 April 2007 Solomon Islands tsunami*. Geophys. Res. Lett., *35*, L01607, doi:10.1029/2007GL031654.

FRITZ, H.M., BLOUNT, C.D., THWIN, S., THU, M.K. and CHAN, N. (2009). *Cyclone Nargis storm surge in Myanmar* Nature Geosci. *2*(7), 448–449, doi:10.1038/ngeo558.

FRITZ, H.M., PETROFF, C.M., CATALAN, P.A., CIENFUEGOS, R., WINCKLER, P., KALLIGERIS, N., WEISS, R., BARRIENTOS, S.E., MENESES, G., VALDERAS-BERMEJO, C., EBELING, C., PAPADOPOULOS, A., CONTRERAS, M., ALMAR, R., DOMINGUEZ, J.C. and SYNOLAKIS, C.E. (2011). *Field Survey of the 27 February 2010 Chile Tsunami*. Pure Appl. Geophys., *168*, 1989–2010.

FRITZ, H.M., PHILLIPS, D.A., OKAYASU, A., SHIMOZONO, T., LIU, H., MOHAMMED, F., SKANAVIS, V., SYNOLAKIS, C.E. and TAKAHASHI, T. (2012). *The 2011 Japan tsunami current velocity measurements* *from survivor videos at Kesennuma Bay using LiDAR*. Geophys. Res. Lett., *39*, L00G23, doi:10.1029/2011GL050686.

Frohlich, C., Hornbach, M.J., Taylor, F.W., Shen, C.C., Moala, A., Morton, A.E. and Kruger, J. (2009). *Huge erratic boulders in Tonga deposited by a prehistoric tsunami*. Geology, *37*(2), 131–134.

Fujii, Y., Satake, K., Sakai, S., Shinohara, M. and Kanazawa, T. (2011). *Tsunami source of the 2011 off the Pacific coast of Tohoku Earthquake*. Earth Planets Space, *63*, 815–820.

Furumura, T., Imai, K. and Maeda, T. (2011). *A revised tsunami source model for the 1707 Hoei earthquake and simulation of tsunami inundation of Ryujin Lake, Kyushu, Japan*. J. Geophys. Res., *116*, B02308, doi:10.1029/2010JB007918.

Hashimoto, C., Noda, A., Sagiya, T. and Matsu'ura, M. (2009). *Interplate seismogenic zones along the Kuril-Japan trench inferred from GPS data inversion*. Nature Geosci., *2*, 141–144.

Hokkaido Tsunami Survey Group (1993). *Tsunami devastates Japanese coastal region*. Eos Trans. AGU, *74*(37), 417–432.

Ide, S., Baltay, A. and Beroza, G.C. (2011). *Shallow dynamic overshoot and energetic deep rupture in the 2011 M_w 9.0 Tohoku-Oki earthquake*. Science, *332*, 1426–1429.

Imamura, F., Goto, K. and Ohkubo, S. (2008). *A numerical model for the transport of a boulder by tsunami*. J. Geophys. Res., *113*, C01008, doi:10.1029/2007JC004170.

Iwate Prefecture (1969). *Reconstruction report for the Chilean earthquake tsunami, Iwate Prefecture*. p. 261. [in Japanese].

JNPA (2011). http://www.47news.jp/CN/201104/CN2011041901000540.html.

JAXA (2011). http://www.satnavi.jaxa.jp/project/alos/news/2011/pdf/110422_alos.pdf.

Kanamori, H. (1972). *Mechanism of tsunami earthquake*. Phys. Earth Planet. Interiors, *6*, 346–359.

Kanamori, H. (1977). *The energy release in great earthquakes*. J. Geophys. Res., *82*, 2981–2987.

Kato, Y. and Kimura M. (1983). *Age and origin of so-called "Tsunami-ishi", Ishigaki island, Okinawa prefecture*. J. Geol. Soc. Jpn, *89*, 471–474.

Liu, H., Takagawa, T., Tajima, Y., Sato, S., Shimozono, T., Okayasu, A. and Fritz, H. M. (2011). *A brief overview on the post-tsunami survey in the Sanriku Coast, Japan*. Proceedings of the 6th Asian and Pacific Coastal Eng. Conf., APAC2011, 91–98.

Liu, P. L.-F., Lynett, P., Fernando, H., Jaffe, B.E., Fritz, H.M., Higman, B., Morton, R., Goff, J. and Synolakis, C. (2005). *Observations by the international tsunami survey team in Sri Lanka*. Science, *308*, 1595.

Matsuo, H. (1933). *Sanriku tsunami survey report*. Rep. Publ. Works Res. Stn., *24*, 83–136. [in Japanese].

MHA (1934). *Reconstruction report of the damaged city after the Sanriku tsunami*. p. 164. [in Japanese].

Mori, N., Takahashi, T. and the 2011 Tohoku Earthquake Tsunami Joint Survey Group (2012). *Nationwide post event survey and analysis of the 2011 Tohoku earthquake tsunami*. Coastal Eng. J., *54*(1), 1250001, doi:10.1142/S0578563412500015.

Munger, S. and Cheung, K.F. (2008). *Resonance in Hawaii waters from the 2006 Kuril Islands tsunami*. Geophys. Res. Lett., *35*, L07605, doi:10.1029/2007GL032843.

Nott, J. (2003). *Waves, coastal boulder deposits and the importance of the pre-transport setting*. Earth and Planetary Sci. Lett., *210*, 269–276.

Ozawa, S., Nishimura, T., Suito, H., Kobayashi, T., Tobita, M. and Imakiire, T. (2011). *Coseismic and postseismic slip of the 2011 magnitude-9 Tohoku-Oki earthquake*. Nature, *475*, 373–376.

Plafker, G. and Savage, J.C. (1970). *Mechanism of the Chilean earthquake of May 21 and 22 1960*. Geol. Soc. Am. Bull., *81*, 1001–1030.

Satake, K. (2005). *Tsunami: Case studies and recent developments.* Springer. p. 351.

Satake, K. and Kanamori, H. (1991). *Abnormal tsunamis caused by the June 13, 1984, Torishima, Japan, Earthquake*. J. Geophys. Res., *96*(B12), 19933–19939.

Sato, M. Ishikawa, T., Ujihara, N., Yoshida, S., Fujita, M., Mochizuki, M. and Asada, A. (2011). *Displacement above the hypocenter of the 2011 Tohoku-Oki earthquake*. Science, *332*, 1395.

Shimozono, T., Sato, S., Okayasu, Y., Tajima, Y., Fritz, H.M., Liu, H. and Takagawa, T. (2012). *Propagation and inundation characteristics of the 2011 Tohoku tsunami on the central Sanriku Coast*. Coastal Eng. J., *54*(1), 1250004, doi: 10.1142/S0578563412500040.

Shuto, N. (1987). *The effectiveness and limit of tsunami control forests*. Coastal Eng. Jpn, *30*(1), 143–153.

Simons, M., Minson, S.E., Sladen, A., Ortega, F., Jiang, J., Owen, S.E., Meng, L., Ampuero, J.-P., Wei, S., Chu, R., Helmberger, D.V., Kanamori, H., Hetland, E., Moore, A.W. and Webb, F.H. (2011). *The 2011 magnitude 9.0 Tohoku-Oki earthquake: mosaicking the megathrust from seconds to centuries*. Science, *332*, 1421–1425.

Tanaka, N., Sasaki, Y., Mowjood, M.I.M., Jinadasa, K.B.S.N. and Homchuen, S. (2007). *Coastal vegetation structures and their functions in tsunami protection: experience of the recent Indian Ocean tsunami*. Landscape Ecol. Eng., *3*, 33–45.

Tanioka, Y. and Satake, K. (1996). *Fault parameters of the 1896 Sanriku Tsunami Earthquake estimated from Tsunami Numerical Modeling*. Geophys. Res. Lett., *23*(13), 1549–1552.

USGS (2011). http://www.usgs.gov/newsroom/article.asp?ID=2727&from=rss_home.

(Received December 7, 2011, revised April 18, 2012, accepted April 20, 2012, Published online June 6, 2012)